

Conformations and Conformational Processes of Hexahydrobenzazocines by NMR and DFT Studies

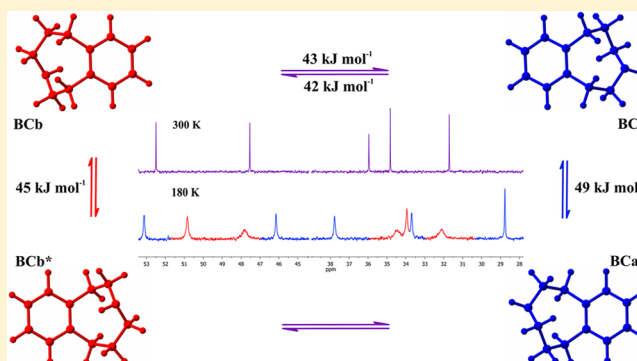
Bogdan Musielak,[†] Tad A. Holak,^{†,‡} and Barbara Rys^{*,†}

[†]Department of Organic Chemistry, Faculty of Chemistry, Jagiellonian University, Ingardena 3, 30-060 Krakow, Poland

[‡]Malopolska Centre for Biotechnology, Jagiellonian University, Gronostajowa 7a, 30-387 Krakow, Poland

S Supporting Information

ABSTRACT: Conformational processes that occur in hexahydrobenzazocines have been studied with the ¹H and ¹³C dynamic nuclear magnetic resonance (DNMR) spectroscopy. The coalescence effects are assigned to two different conformational processes: the ring-inversion of the ground-state conformations and the interconversion between two different conformers. The barriers for these processes are in the range of 42–52 and 42–43 kJ mol⁻¹, respectively. Molecular modeling on the density functional theory (DFT) level and the gauge invariant atomic orbitals (GIAO)-DFT calculations of isotropic shieldings and coupling constants for the set of low-energy conformations were compared with the experimental NMR data. The ground-state of all compounds in solution is the boat–chair (BC) conformation. The BC form adopts two different conformations because the nitrogen atom can be in the boat or chair parts of the BC structure. These two conformers are engaged in the interconversion process.



INTRODUCTION

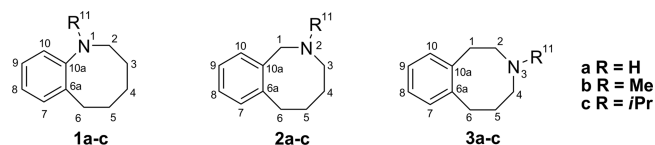
Organic compounds that contain the N-heterocyclic eight-membered ring have mostly been considered as potential drugs due to their affinity for the opioid receptor and their structural similarity to the benzomorphan system.¹ Modification of the structure of these compounds, by introducing an oxygen atom to the heterocyclic ring, retains analgesic properties, and these structures are classified as non-narcotic analgesics.² Benzazocines have been shown to have antitumor activity³ and also can be effective against the HIV virus.⁴

One of the main methods used for studying the conformational behavior of cyclic chemical systems is the variable-temperature (VT) NMR spectroscopy combined with prediction of NMR parameters derived from the computationally generated conformers using the -gauge invariant atomic orbitals-density functional theory (GIAO-DFT) calculations. Azacyclooctane is the simplest eight-membered ring which contains the nitrogen atom and conformational studies by the dynamic ¹³C NMR showed that azacyclooctane adopts the boat–chair (BC) and crown conformations in solution. Differences in the energies between the BC and crown conformers is $\Delta E = 5$ kJ mol⁻¹ and the barrier of interconversion is $\Delta G^\ddagger = 44$ kJ mol⁻¹.⁵ For the BC conformation, the barrier for the ring inversion, which is equal $\Delta G^\ddagger = 31$ kJ mol⁻¹, was also established.⁵ The dominating BC conformation was observed for the N-methyl and N-tosyl derivatives.⁶ Favored conformations for benzazocinone derivatives studied with VT NMR are the twist–boat–chair, BC, and twist–boat conformations. The energy barriers

are in the range 38–100 and 36–105 kJ mol⁻¹ for the inversion and interconversion processes, respectively.⁷ Studies carried out using DNMR and X-ray of the benzo[b]azocines with the N-benzoyl moiety showed that these derivatives adopt the BC conformation in both solution and solid states, and the activation energy for the ring inversion is in the range of 69.9–71.1 kJ mol⁻¹.⁸ In the case of dibenzoazocine the preferred conformations are different, and their geometry depends on the N-substituent and on the localization of benzene rings. These molecules can adopt the BC, twist–boat, boat, and chair forms.⁹ Conformational processes in 2,5-benzoxazocine derivatives studied by Glaser showed that nefopan adopts only the boat–boat (BB) and twist–chair–chair (TCC) states.¹⁰

In the present investigation, the conformational behavior of benzazocine derivatives **1–3** (Scheme 1) has been described.

Scheme 1. Structure of the Investigating Compounds with the Numbering Scheme^a



^aThe numbering does not correspond to the IUPAC nomenclature. This is done for the sake of better comparability of the systems.

Received: July 21, 2015

Published: August 28, 2015

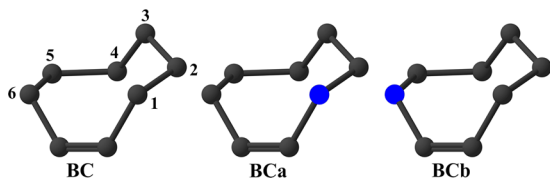
The preferred ground-state conformations in the solution were explored with the dynamic ^1H and ^{13}C NMR spectroscopy and by molecular modeling methods carried out at the density functional theory (DFT) level.

RESULTS AND DISCUSSION

Synthesis. All isomers of benzazocines were synthesized by the reduction of appropriate benzazocinones with lithium aluminum hydride in ethyl ether. Lactams were obtained by the Schmidt reaction of a ketone with sodium azide in the acidic condition.^{7a} Their *N*-alkyl derivatives were prepared by the reaction of lactams with methyl iodide or isopropyl bromide (4) in the presence of sodium hydride in the DMF solution. The *N*-isopropyl derivatives (5,6) were synthesized according to the procedure described by Johnstone.¹¹

Nomenclature of Conformers. The conformational terminology for the medium-sized rings proposed by Hendrickson is used throughout the paper.¹² For the parent hydrocarbon, *cis*-cyclooctene, two conformers BC and BB were found.¹³ However, replacement of the methylene group at C-1 or C-6 by nitrogen in the BC conformer of the carbocyclic ring leads to two different conformations (Scheme 2). The same is

Scheme 2. BC Conformations of *cis*-Cyclooctene and Hexahydroazocine



true for the bezoannulated analogues 1–3 and for other conformations of the eight membered-ring. To distinguish the

two different spatial arrangements of the nitrogen atom, suffix (a) or (b) is added to the descriptor of the conformation (the former corresponds to the substitution of the carbon atom with its lower number).

Dynamic NMR Studies and Conformational Processes.

All ^1H NMR signals of 1a–c become broadened with decreasing temperature. Their coalescences are observed at 180 K for 1a, in the range of 220–200 K for 1b, and for the compound with the isopropyl substituent at the nitrogen atom at 240–200 K (Figure 1, Supporting Information Figures S25 and S27). The signals become sharp below the coalescence temperature only for the *N*-alkylated compounds, and in the case of 1a the signals were still broadened at these temperatures.

The changes in line shapes of the NMR signals are also observed between 300 and 170 K in the ^{13}C NMR spectra of 1a,b (Supporting Information Figures S26 and S28). Lowering the temperature causes broadening of all carbon signals. ^{13}C spectra of 1c show sharp signals throughout the range of temperatures, with the exception of the signal from carbons C-12 and C-13 ($\delta = 22.6$ ppm at 300 K), which split into two signals below 200 K (Figure 2). The assignment of the proton and carbon signals was carried out using the COSY, HSQC, and HMBC spectra recorded at 300 K and at the lowest temperature of the temperature-dependent measurements.

The data above can be interpreted as follows: the molecules are frozen in their chiral ground-state conformations at 170 K. The racemization of the chiral eight-membered ring, during which hydrogen atoms in methylene groups interconvert their stereochemical positions, occurs on raising the temperature. Furthermore, another conformational process for 1a and 1b, namely the interconversion between two different conformations, can also be considered, but in neither ^1H nor ^{13}C NMR spectra the presence of the second conformer could be detected.

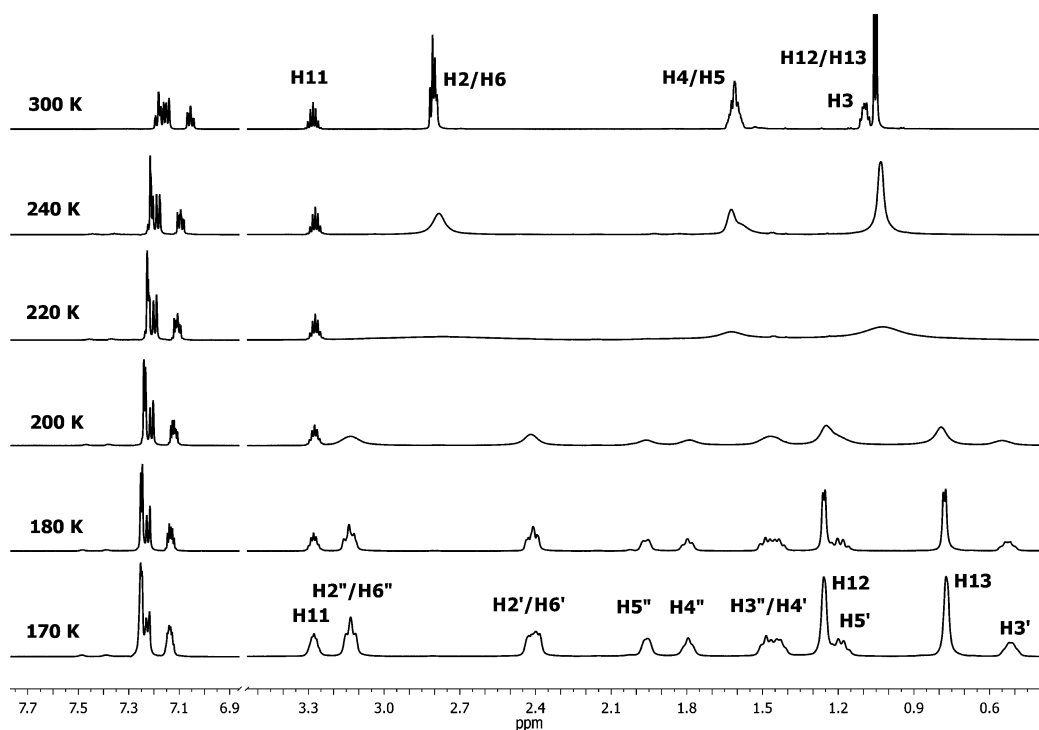


Figure 1. Temperature dependence of ^1H NMR spectra of 1c in CD_2Cl_2 (300–170 K).

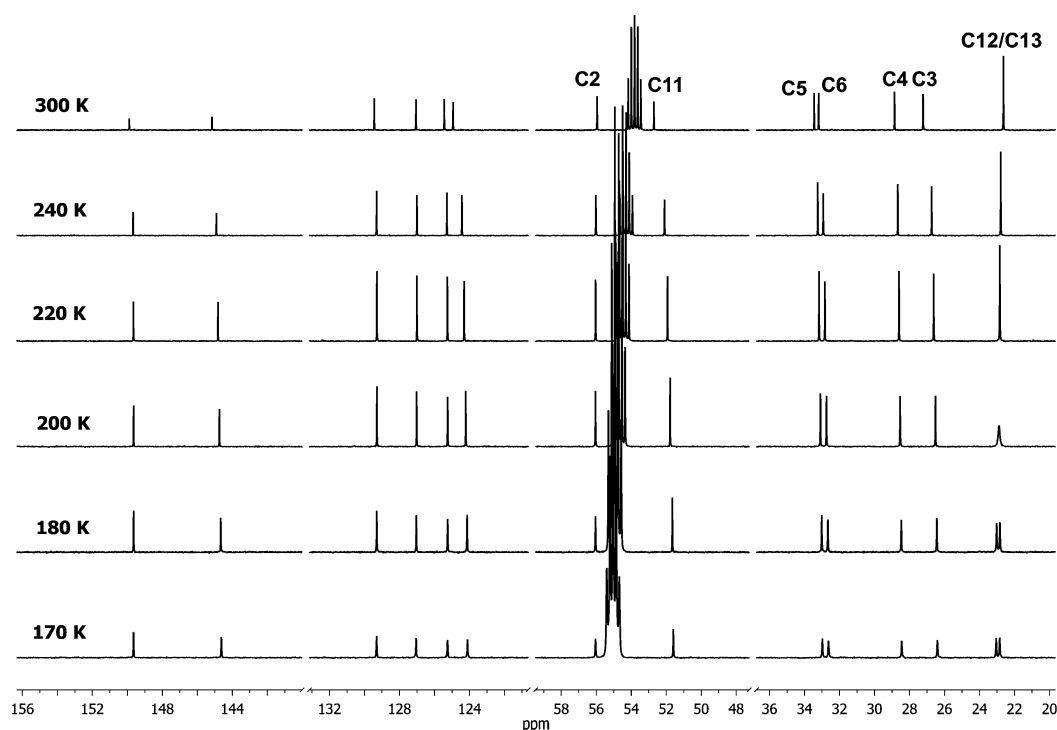


Figure 2. Temperature dependence of ^{13}C NMR spectra of **1c** in CD_2Cl_2 (300–170 K).

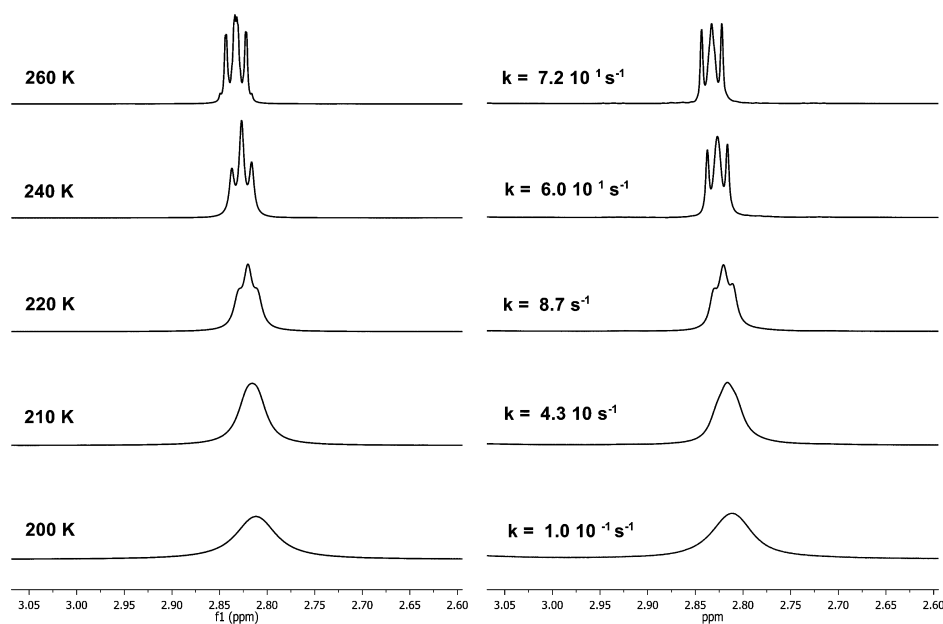


Figure 3. Experimental (left) and fitted (right) line shapes of the H6 proton along with the calculated rates (s^{-1}) obtained from the ^1H DNMR measurements for **1a** in CD_2Cl_2 .

Table 1. Experimental Barriers for Dynamic Processes (kJ mol^{-1}) in Molecules **1–3** from DNMR

| compound | 1a | 1b | 1c | 2a | 2b | 2c | 3a | | 3b | | 3c |
|-------------------------|------------|------------|------------|------------|------------|-----------|------------------------|---------------------|---------------------|------------------------|---------------------|
| inversion barrier | 51 ± 2 | 45 ± 2 | 46 ± 2 | 44 ± 2 | 43 ± 1 | – | major 45 ± 2 | minor 49 ± 5 | major 42 ± 1 | major 48 ± 2 | minor 52 ± 1 |
| interconversion barrier | | | | | | | major→minor 43 ± 1 | | | major→minor 43 ± 1 | |
| | | | | | | | minor→major 42 ± 1 | | | minor→major 43 ± 1 | |

The estimation of free energy barriers for the observed ring inversion processes is illustrated in Figure 3 where the temperature dependence of the H6 signal with the rate

constant is shown. The free enthalpy of activation is calculated based on the Eyring equation and are $\Delta G^\ddagger = 51$, 45, and 46 kJ mol^{-1} for **1a**, **1b**, and **1c**, respectively. The values of the energy

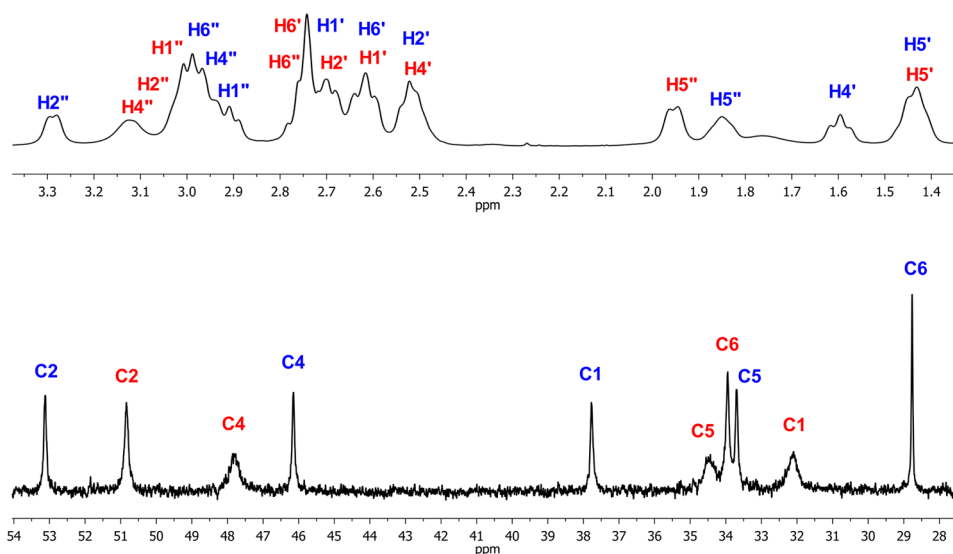


Figure 4. ^1H and ^{13}C NMR spectra of two conformers of **3a** in the CD_2Cl_2 solution at 180 K. The assignments of the signals from the major and minor conformers are marked in red and blue, respectively.

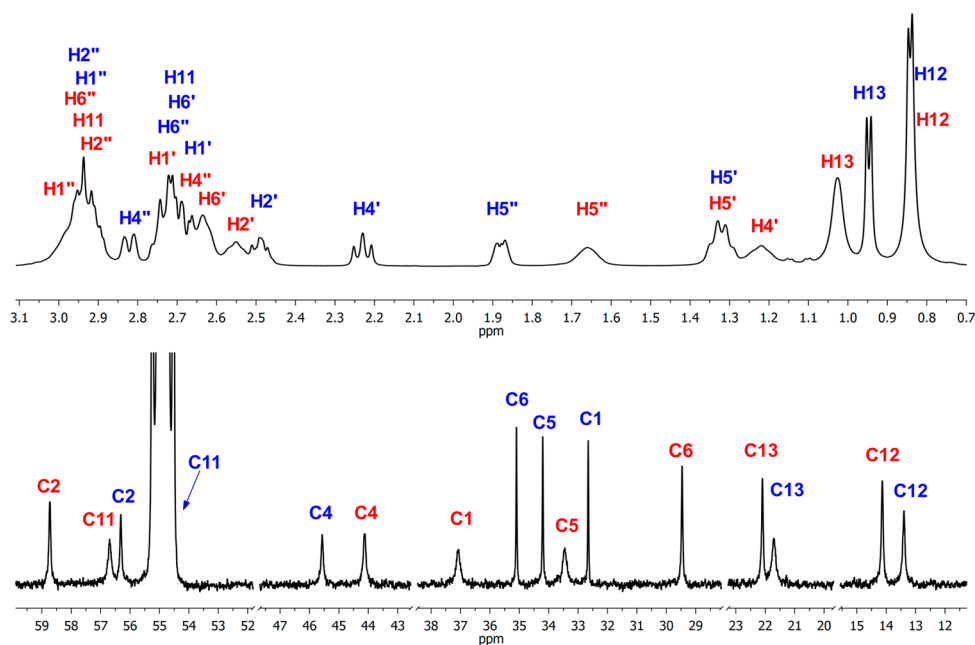


Figure 5. ^1H and ^{13}C NMR spectra of two conformers of **3c** in CD_2Cl_2 at 180 K. The assignments of the signals from the major and minor conformers are marked in red and blue, respectively.

barriers of conformational processes for the investigated hexahydrobenzazocines are summarized in Table 1.

Coalescence processes are observed in hexahydrobenzo[*c*]-azocines **2** in both ^1H and ^{13}C NMR spectra. Changes in the line shapes are seen for all signals. The signals of **2a** and **2c** are still broaden in the NMR spectra at the lowest temperature. This is in contrast to those of **2b**, for which sharp and well-separated signals are seen at 170 K (Supporting Information Figures S31–S36). Our interpretation of these observations is that lowering the temperature reduces the rate of the inversion of the major conformer of the N-heterocyclic ring in **2**'s. This process is accompanied by a second process which is the interconversion between two different conformers. The difference in the energy between the two conformers is too high for **2a** and **2c** for the NMR signals of the higher energy conformer

to be seen in the NMR spectra at these temperatures. This is in contrast to **2b** for which the energy difference between two conformers is sufficiently low resulting in the observance the signals in both the ^1H and ^{13}C NMR spectra at 170 K. The split in the ^1H spectral signals of the lower populated conformer reveals that the process of interconversion of the minor conformer is inhibited. The ratio of the conformers at 170 K is equal 2:1 (determined from the ^1H NMR spectra). The energy barriers of the eight-membered-ring inversion of **2a,b** are similar, and they are equal to approximately $43\text{--}44\text{ kJ mol}^{-1}$ (Table 1).

The line-shapes of the NMR signals in both ^1H and ^{13}C NMR spectra were monitored for all hexahydrobenzo[*d*]-azocines (Supporting Information Figures S37–S42). All aliphatic carbon resonances are broadened in the spectra

recorded at 300 K, and with the temperature lowering they split into two nearly equally intense signals in the spectra of **3a** and **3c**. Only one set of sharp signals is observed for **3b**, and there is no evidence of the existence of the second conformer even at temperatures lower than 180 K. In contrast to the carbon spectra, there is a raised baseline in the ^1H NMR in the range $\delta = 7.33\text{--}7.00$ and $3.60\text{--}1.15$ ppm at 180 K, which suggests the presence of the second conformer. Distribution of the conformers for compounds **3a** and **3c** is 1:0.8 (Figures 4 and 5). The multiplet at $\delta = 1.68$ ppm (H-5) of **3a** (Supporting Information Figure S37) in the spectra measured at 300 K splits into three signals at 180 K, whereas the signal at $\delta = 1.43$ ppm is a combination of two signals from the H5'-protons of different conformers. The signals of H5 for the first conformer are at $\delta = 1.43$ and 1.95 ppm and correlate with the signal at $\delta = 34.2$ ppm in the HSQC spectrum, while for the second one they are at $\delta = 1.43$ and 1.85 ppm and they connect to the signal at $\delta = 33.7$ ppm of the HSQC spectrum (Supporting Information Figure S43). Separate signals of the diastereotopic protons of both conformers are present in the proton spectra (i.e., the protons are magnetically nonequivalent). This spectral feature can be interpreted similarly to that for **2**: the inversion of the ground-state conformation and the interconversion between two different conformers. A similar situation is observed in the NMR spectra of **3c** (Supporting Information Figure S44). The energy barriers for the conformational processes in **3** are summarized in Table 1.

Computational Studies. The conformational space of the molecules of hexahydrobenzazocines was explored using the DFT with the hybrid B3LYP functional using 6-311G++(d,p) basis sets in energy window of 40 kJ mol $^{-1}$. Theoretical chemical shifts of ^1H and ^{13}C nuclei were calculated for all conformers using the DFT-GIAO at the same combination of functional and basis sets. That the five conformers of **1a** have the population above 1% (Supporting Information Table S2). Energy difference between two lowest-energy minima is equal $\Delta E = 1.22$ kJ mol $^{-1}$ for isolated molecules and $\Delta E = 0.94$ kJ mol $^{-1}$ in dichloromethane. However, the population of the first conformer (BCb) was approximately 15% lower than that of the BBa. This difference is due to the fact that the free energy value of the second conformer is less than the first. The calculations performed for **1b** and **1c** showed that their conformational space is not complicated and the global minima of the BCb are well separated from all other conformers, leading to the population higher than 90% for the BCb. Three rotamers were found for the dominant conformer **1c**, which have different energies depending on the position of the isopropyl substituent at the nitrogen atom. The lowest-energy conformation adopted by **1** is virtually the same and can be described as the boat-chair (BCb) (Figure 6). This was established by comparing the endocyclic dihedral angles of *cis*-

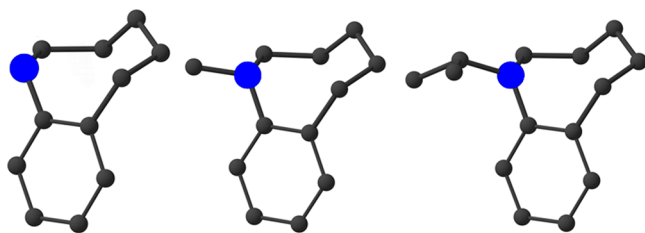


Figure 6. Lowest-energy conformers BCb of **1a** (left), **1b** (center), and **1c** (right) as calculated by the DFT methods.

cyclooctene and benzazocines **1** (Supporting Information Table S1). It is worth noting that the twist-chair (TC) conformation found in **1a**, populated at 6% in the “solvent model”, has not been found for *cis*-cyclooctene (Supporting Information Table S2).

The calculated ^1H and ^{13}C spectral NMR parameters of the lowest-energy BCb of **1** are in good agreement with the experimental NMR data. The correlation coefficients are 0.9984 and 0.9987 for proton NMR spectra of **1a,c** and **1b**, respectively. The largest discrepancy between the calculated and experimental chemical shifts has not exceeded 0.20 ppm, with the average difference smaller than 0.08 ppm. Similarly, close agreement has been found for the ^{13}C NMR chemical shifts (Supporting Information Tables S11–S14). Thus, the matching of the calculated and experimental spectra allowed us to postulate that the conformation observed in the solution for molecules **1** are the same as the global minimum, i.e., the BCb conformation, found by molecular modeling. Additional arguments for validation of the BCb conformation came from the coupling constants in the proton NMR spectra. Simulation of the line shapes of the aliphatic signals in the ^1H spectrum of **1b** at 180 K (using program from the TopSpin package)¹⁴ allowed accurate determination of the experimental geminal and vicinal coupling constants and their comparison with calculated values (Table 2). The analysis performed for the

Table 2. Comparison of the Values of Coupling Constants obtained from ^1H NMR spectra (J_{exp}) and Calculated (J_{calcd}) using the GIAO/DFT Method for the BCb Conformer of **1b**

| hydrogen atom | J_{exp} (Hz) | J_{calcd} (Hz) |
|---------------|--|--|
| H3' | $^2J = 15.1; ^3J = 13.9; 9.0; 5.7; 4.1$ | $^2J = 13.9; ^3J = 11.4; 8.1; 4.0; 0.4$ |
| H3'' | $^2J = 15.1; ^3J = 11.1; 3.2; 0.0; 0.0$ | $^2J = 13.9; ^3J = 9.8; 4.1; 2.3; 0.4$ |
| H4' | $^2J = 14.8; ^3J = 14.7; 9.0; 3.9; 3.2$ | $^2J = 13.2; ^3J = 11.2; 8.1; 3.0; 0.4$ |
| H4'' | $^2J = 14.8; ^3J = 11.1; 4.3; 4.1; 3.0$ | $^2J = 13.2; ^3J = 9.8; 3.9; 3.3; 0.4$ |
| H5' | $^2J = 14.8; ^3J = 14.7; 11.1; 3.0; 1.6$ | $^2J = 12.7; ^3J = 11.2; 11.1; 3.3; 1.7$ |
| H5'' | $^2J = 14.8; ^3J = 4.3; 4.2; 4.2; 3.9$ | $^2J = 12.7; ^3J = 6.1; 3.9; 3.0; 1.8$ |

NMR signals shows that the whole set of coupling constants is in excellent agreement with the geometry of the global minimum conformation of **1b** found by the DFT calculation. The small differences between the values of the calculated and experimental coupling constants may result from the broadening of the signals due at the decreased temperature and increased viscosity of the solvent.

In the ^1H NMR spectra chemical shift of proton H3' is observed at the lower frequency when increasing the steric bulkiness at the nitrogen atom (**1a** $\delta_{\text{H}3'} = 1.03$ ppm, **1b** $\delta_{\text{H}3'} = 0.65$ ppm, and **1c** $\delta_{\text{H}3'} = 0.53$ ppm) because of the steric hindrance forces the H3' atom above the aromatic ring, thereby a ring current effect shields atoms H3'.

Our molecular modeling predicted that the lowest-energy conformation of compound **2** in the solution is the BC form (Supporting Information Figures S53–S55). In the case of **2a** and **2c** the conformers that are preferred are those of the BCa form, while in **2b** this is the BCb conformation. Comparison of the spectral NMR parameters obtained for the experiments at the lowest temperature and calculated data for compounds **2a**

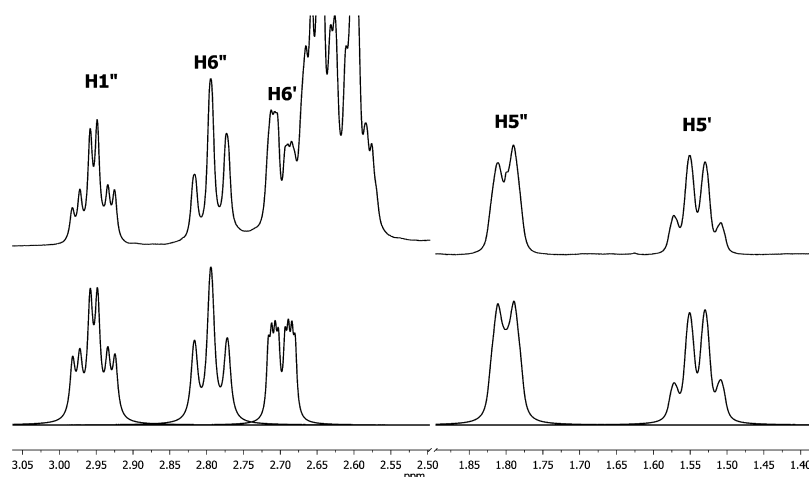


Figure 7. Aliphatic parts of the experimental (above) and fitted (below) ^1H NMR spectra of **3b**.

and **2c** was not possible; therefore the experimental parameters extracted from the spectra measured at 300 K can be used (Supporting Information Tables S15, S16, S21, and S22). These calculated data were compared with the experimental chemical shifts both individually and as the Boltzmann-weighted averages. Based on this comparison it has been established that the investigated structures are involved in the fast conformational processes leading to the time-averaged spectra. The equilibrium of compound **2a** contains conformers BCa and BCb, while **2c** contains BCa, BBa, and BCb. In both **2a** and **2c** the BCa conformation dominates (the remaining conformers are below 10% and do not introduce significant changes in this statistical evaluation). The assignment of the major conformer for **2b** was straightforward. The spectra calculated for the BCb conformers of **2b** gave the best agreement with the experimental data obtained at 170 K (Supporting Information Tables S17 and S18). Determination of the minor conformer of **2b** was impossible because the set of NMR signals was incomplete in the spectra due to signal overlap. Therefore, the calculated shielding constants are compared with the chemical shifts at 300 K. The best statistical fit was achieved when the spectral parameters used came from conformers BCb and BCa (Supporting Information Tables S19 and S20). We conclude that in the NMR spectra at 300 K the averaged signals from conformations BCb and BCa are observed.

Conformational modeling showed that both the BCa and BCb conformations are preferred by compounds **3** (Supporting Information Figures S56–S58). The geometry optimization with the solvent effect gives very small differences in the ΔG between the BCa and BCb forms ($\Delta G = 0.63$, -0.06 , and 0.59 kJ mol^{-1} for **3a**, **3b**, and **3c**, respectively), thus their populations are very similar (Supporting Information Tables S8–S10). The spectra calculated for these conformers gave the best agreement with the experimental chemical shifts of the major conformers for the BCb form in the case of **3a** and **3b** and of the minor conformer for the BCa in **3a** (Supporting Information Tables S23–S25). For compound **3c**, both the theoretical and experimental calculations are consistent, and the major conformer observed in the NMR spectra adopted the BCa, while a minor the BCb conformation (Supporting Information Tables S26 and S27).

Additional validation of the BCa and BCb conformations comes from the comparison of the differences between

chemical shifts and shielding constants of their geminal protons. For example, the largest difference (above 1 ppm) is observed for signals H4 of the minor conformer **3a** ($\Delta\delta_{\text{H4}} = 1.36$ ppm) and major **3c** ($\Delta\delta_{\text{H4}} = 1.43$ ppm). We also found similar values $\Delta\sigma_{\text{H4}}$ for the BCa conformations, which is 1.19 and 1.11 for **3a** and **3c**, respectively. In the case of compound **3b** we have additional evidence which allowed the correct assignment of the conformation BCb in the NMR spectra. This is the comparison of the geminal and vicinal coupling constants of the isolated proton signals of **3b** in the ^1H spectrum with the predicted values obtained from the GIAO-DFT calculation. Agreement between these two series is excellent (Figure 7 and Table 3).

SUMMARY REMARKS

The structures and conformations of hexahydrobenzazocines **1–3** were determined by variable-temperature NMR spectroscopy.

Table 3. Comparison of the Values of Geminal and Vicinal Coupling Constants from Experimental and Calculated by DFT method Spectra for BC Conformers of **3b**

| hydrogen atom | BCb _{exp} J_{exp} (Hz) | BCb _{calcd} J_{calcd} (Hz) | BCa _{calcd} J_{calcd} (Hz) |
|---------------|--|--|--|
| H1'' | $^2J_{\text{H1}''\text{-H1}'} = 14.4$ | $^2J_{\text{H1}''\text{-H1}'} = 12.6$ | $^2J_{\text{H1}''\text{-H1}'} = 12.8$ |
| | $^3J_{\text{H1}''\text{-H2}'} = 6.0$ | $^3J_{\text{H1}''\text{-H2}'} = 5.5$ | $^3J_{\text{H1}''\text{-H2}'} = 14.3$ |
| | $^3J_{\text{H1}''\text{-H2}''} = 14.4$ | $^3J_{\text{H1}''\text{-H2}''} = 11.5$ | $^3J_{\text{H1}''\text{-H2}''} = 5.4$ |
| H6'' | $^2J_{\text{H6}''\text{-H6}'} = 13.9$ | $^2J_{\text{H6}''\text{-H6}'} = 12.7$ | $^2J_{\text{H6}''\text{-H6}'} = 11.8$ |
| | $^3J_{\text{H6}''\text{-H5}'} = 13.0$ | $^3J_{\text{H6}''\text{-H5}'} = 11.2$ | $^3J_{\text{H6}''\text{-H5}'} = 11.2$ |
| | $^3J_{\text{H6}''\text{-H5}''} = 1.9$ | $^3J_{\text{H6}''\text{-H5}''} = 2.3$ | $^3J_{\text{H6}''\text{-H5}''} = 5.1$ |
| H6' | $^2J_{\text{H6}'\text{-H6}''} = 13.9$ | $^2J_{\text{H6}'\text{-H6}''} = 12.7$ | $^2J_{\text{H6}'\text{-H6}''} = 11.8$ |
| | $^3J_{\text{H6}'\text{-H5}'} = 2.4$ | $^3J_{\text{H6}'\text{-H5}'} = 2.2$ | $^3J_{\text{H6}'\text{-H5}'} = 5.3$ |
| | $^3J_{\text{H6}'\text{-H5}''} = 5.1$ | $^3J_{\text{H6}'\text{-H5}''} = 5.5$ | $^3J_{\text{H6}'\text{-H5}''} = 2.2$ |
| H5'' | $^2J_{\text{H5}''\text{-H4}'} = 13.4$ | $^2J_{\text{H5}''\text{-H4}'} = 12.5$ | $^2J_{\text{H5}''\text{-H4}'} = 12.1$ |
| | $^3J_{\text{H5}''\text{-H4}''} = 2.0$ | $^3J_{\text{H5}''\text{-H4}''} = 1.5$ | $^3J_{\text{H5}''\text{-H4}''} = 4.9$ |
| | $^3J_{\text{H5}''\text{-H4}'} = 4.5$ | $^3J_{\text{H5}''\text{-H4}'} = 4.1$ | $^3J_{\text{H5}''\text{-H4}'} = 11.4$ |
| | $^3J_{\text{H5}''\text{-H6}'} = 5.1$ | $^3J_{\text{H5}''\text{-H6}'} = 5.5$ | $^3J_{\text{H5}''\text{-H6}'} = 2.2$ |
| H5' | $^3J_{\text{H5}'\text{-H6}''} = 1.9$ | $^3J_{\text{H5}'\text{-H6}''} = 2.3$ | $^3J_{\text{H5}'\text{-H6}''} = 5.1$ |
| | $^2J_{\text{H5}'\text{-H5}''} = 13.4$ | $^2J_{\text{H5}'\text{-H5}''} = 12.5$ | $^2J_{\text{H5}'\text{-H5}''} = 12.1$ |
| | $^3J_{\text{H5}'\text{-H4}''} = 11.8$ | $^3J_{\text{H5}'\text{-H4}''} = 10.5$ | $^3J_{\text{H5}'\text{-H4}''} = 2.1$ |
| | $^3J_{\text{H5}'\text{-H4}'} = 3.3$ | $^3J_{\text{H5}'\text{-H4}'} = 3.0$ | $^3J_{\text{H5}'\text{-H4}'} = 3.0$ |
| | $^3J_{\text{H5}'\text{-H6}'} = 2.4$ | $^3J_{\text{H5}'\text{-H6}'} = 2.2$ | $^3J_{\text{H5}'\text{-H6}'} = 5.3$ |
| | $^3J_{\text{H5}'\text{-H6}''} = 13.0$ | $^3J_{\text{H5}'\text{-H6}''} = 11.2$ | $^3J_{\text{H5}'\text{-H6}''} = 11.2$ |

copy and the DFT computations. The calculated data of the individual conformers and the Boltzmann-weighted averages of the conformers were compared with the GIAO calculation of the ^1H and ^{13}C NMR chemical shifts and homonuclear coupling constants $J_{\text{H-H}}$. The excellent agreement between the experimental and the predicted data allowed the establishment of the ground-state conformations in solution for all investigated compounds. The dynamic NMR was used to determine the activation energy of the conformational processes in the N-heterocyclic eight-membered ring.

Conformations of all of the compounds adopt the BC structures similar to that seen in *cis*-cyclooctene. The benzoannulation of the aliphatic ring and the localization of the nitrogen atom in the core scaffold do not influence their conformations. The conformation TC (conformer 4–6% of population) was found for compound **1a**. Such a local energy minimum was not seen in *cis*-cyclooctene. The *N*-alkyl substituent in hexahydrobenzazocine does not change the geometry of the eight-membered ring.

Only compound **1c** does not show the spectral processes related to the interconversion between two different BCa and BCb conformers. The activation energy of the racemization of the ground-state conformation are from 42 to 52 kJ mol^{-1} , and they are higher than for azacyclooctanes.⁵ The energy barrier for the interconversion processes is in the range 42–43 kJ mol^{-1} .

EXPERIMENTAL SECTION

General Procedures. TLC was carried out on SiO_2 and was visualized by UV light (254 nm) or iodine. Column chromatography was performed on silica gel 60 (0.040–0.063 mm). Melting points were uncorrected. IR spectra were recorded by ATR methods. Mass spectral data were reported in m/z .

Benzazocinones and their *N*-alkylated derivatives were prepared according to reported procedures.^{7a,11}

1-Isopropyl-3,4,5,6-tetrahydro-1H-benzo[b]azocin-2-one (4). Using 0.70 g (4.0 mmol, 1 equiv) 3,4,5,6-tetrahydro-1H-benzo[b]azocin-2-one, 0.20 g (5.2 mmol, 1.3 equiv) NaH and 0.75 mL (8.0 mmol, 2.0 equiv) isopropyl bromide provided 1-isopropyl-3,4,5,6-tetrahydro-1H-benzo[b]azocin-2-one (0.66 g, 76%) as a colorless crystals; mp 73–74 °C (hexane); R_f = 0.43 (SiO_2 /ethyl acetate); IR (ATR): 2981, 2962, 2943, 1861, 1637, 1489, 1447, 1394, 1362, 1362, 1342, 1303, 1260, 1126, 1039, 767 cm^{-1} ; ^1H NMR (600 MHz, CDCl_3), δ : 0.91 (d, 3H, 3J = 6.8 Hz, H12), 1.33–1.38 (m, 1H, H5'), 1.35 (d, 3H, 3J = 6.8 Hz, H-13), 1.75–1.83 (m, 1H, H4'), 1.82–1.89 (m, 1H, H4''), 1.91 (td, 1H, 3J = 12.1 Hz, 4J = 1.5 Hz, H3'), 2.08–2.13 (m, 1H, H5''), 2.22 (ddd, 1H, 3J = 12.1 Hz, 3J = 7.9 Hz, 3J = 1.2 Hz, H3''), 2.45 (td, 1H, 3J = 13.3 Hz, 3J = 1.2 Hz, H6'), 2.73 (dd, 1H, 3J = 13.3 Hz, 3J = 7.1 Hz, H6''), 4.99 (septet, 1H, 3J = 6.8 Hz, H11), 7.14 (d, 1H, 3J = 7.8 Hz, H10), 7.19–7.24 (m, 1H, 3J = 5.5 Hz; 4J = 3.1 Hz, H9), 7.27–7.31 (m, 2H, H7/9); ^{13}C NMR (151 MHz, CDCl_3), δ : 19.4 (C12), 22.6 (C13), 25.7 (C4), 29.9 (C5), 31.0 (C6), 34.0 (C3), 47.4 (C11), 126.5 (C9), 127.2 (C10), 128.4 (C8), 130.5 (C7), 138.5 (C10a), 142.6 (C6a), 174.3 (C2); MS m/z = 217 [M^+]; Anal. calcd for $\text{C}_{14}\text{H}_{19}\text{NO}$: C, 77.38; H, 8.81; N, 6.45; Found: C, 77.17; H, 8.80; N, 6.61.

2-Isopropyl-1,4,5,6-tetrahydro-2H-benzo[c]azocin-3-one (5). Using 0.29 g (1.7 mmol, 1 equiv) 1,4,5,6-tetrahydro-2H-benzo[c]azocin-3-one, 0.28 g (6.8 mmol, 4 equiv) potassium hydroxide and 0.32 mL (3.4 mmol, 2.0 equiv) isopropyl bromide provided 2-isopropyl-1,4,5,6-tetrahydro-2H-benzo[c]azocin-3-one (0.11 g, 31%) as a colorless oil; R_f = 0.34 (SiO_2 /ethyl acetate); IR (ATR): 3062, 2969, 2932, 2868, 1631, 1451, 1420, 1363, 1215, 747 cm^{-1} ; ^1H NMR (600 MHz, CDCl_3), δ : 1.13–1.14 (d, 6H, 3J = 6.9 Hz, H-12 and H-13), 2.03 (br, 2H, H-5), 2.66 (t, 2H, 3J = 6.6 Hz, H-4), 2.88 (t, 2H, 3J = 5.9 Hz, H-6), 4.53 (br s, 2H, H-1), 4.63 (br, 1H, H-11), 7.11–7.12

and 7.17–7.19 (m, 4H, H-Ar), ^{13}C NMR (151 MHz, CDCl_3), δ : 20.3 (C-12 and C-13), 26.9 (C-5), 34.2 (C-6), 35.6 (C-4), 47.0 (C-11), 48.9 (C-1), 126.6, 127.6, 128.7, 131.9 (C-7 – C-10), 137.7 and 140.6 (C-6a and C-10a); MS m/z = 217 [M^+]; HRMS (ESI-TOF) m/z calcd for $\text{C}_{14}\text{H}_{20}\text{NO}$ 218.1539; found: 218.1553 [$\text{M} + \text{H}^+$].

3-Isopropyl-3,4,5,6-tetrahydro-1H-benzo[d]azocin-2-one (6). Using 0.35 g (2.5 mmol, 1 equiv) 3,4,5,6-tetrahydro-1H-benzo[d]azocin-2-one, 0.45 g (8.0 mmol, 4 equiv) potassium hydroxide and 0.38 mL (4.0 mmol, 2.0 equiv) isopropyl bromide provided 3-isopropyl-3,4,5,6-tetrahydro-1H-benzo[d]azocin-2-one (0.12 g, 28%) as a colorless crystals; mp 113–114 °C (cyclohexane) R_f = 0.34 (SiO_2 /ethyl acetate/petroleum ether (40–60) 5:1); IR (ATR): 3062, 3018, 2974, 2937, 2859, 1620, 1488, 1455, 1419 cm^{-1} ; ^1H NMR (600 MHz, $\text{CDCl}_2\text{CDCl}_2$, 360 K), δ : 1.00 (d, 6H, 3J = 6.8 Hz, H-12 and H-13), 1.80 (br, 2H, H-5), 2.89 (dd, 2H, 3J = 6.2 Hz, 3J = 5.3 Hz, H-6), 3.45 (t, 2H, 3J = 5.1 Hz, H-4), 3.68 (br, 2H, H-1), 4.59 (septet, 1H, 3J = 6.8 Hz, H-11), 7.07 (dd, 1H, 3J = 6.5 Hz, 4J = 2.4 Hz, H-7), 7.11–7.15 (m, 2H, H-8 and H-9), 7.32 (dd, 1H, 3J = 6.5 Hz, 4J = 2.4 Hz, H-10), ^{13}C NMR (151 MHz, $\text{CDCl}_2\text{CDCl}_2$, 360 K), δ : 20.0 (C-12 and C-13), 32.4 (C-5), 36.0 (C-6), 41.5 (C-1), 44.2 (C-4), 45.3 (C-11), 129.7 (C-7), 127.2 and 126.8 (C-8 and C-9), 130.1 (C-10), 136.2 and 140.1 (C-6a and C-10a), 172.2 (C-2); MS m/z = 217 [M^+]; Anal. calcd for $\text{C}_{14}\text{H}_{19}\text{NO}$: C, 77.38; H, 8.81; N, 6.45; Found: C, 77.30; H, 8.86; N, 6.62.

General Method Synthesis of Benzazocines. To the suspension of LiAlH_4 (2 equiv) in dry ethyl ether lactam (1 equiv) was added in portions at 0 °C. After the mixture was stirred at 0 °C for 30 min, the reaction was allowed to warm to room temperature and then heated to reflux for 10 h. After this time, the mixture was cooled in an ice-bath and quenched by the addition of water and 15% aqueous NaOH. The inorganic solid was filtered off and washed with ethyl ether. The ethereal filtrate was dried over potassium hydroxide and evaporated. The residue was chromatographed on silica gel and molecular distilled.

1,2,3,4,5,6-Hexahydrobenzo[b]azocine (1a). Using 0.78 g (4.6 mmol, 1 equiv) 3,4,5,6-tetrahydro-1H-benzo[b]azocin-2-one and 0.35 g (9.2 mmol, 2 equiv) LiAlH_4 provided compound **1a** (0.63 g, 88%) as a colorless oil; bp 70–75 °C/0.05 mmHg (lit.¹⁵ bp 130–150 °C/15 mmHg); R_f = 0.42 (Al_2O_3 /dichloromethane); IR (ATR): 3417, 3336, 3050, 3011, 2926, 2848, 1603, 1493, 1453, 743 cm^{-1} ; ^1H NMR (600 MHz, CD_2Cl_2), δ : 1.49–1.55 (m, 4H, H-3, H-4), 1.70–1.74 (m, H-5), 2.85 (t, 2H, 3J = 6.4 Hz, H-6), 3.21 (t, 2H, 3J = 5.5 Hz, H-2), 3.79 (br, 1H, H-1 (NH)), 6.85 (dd, 1H, 3J = 7.5 Hz; 4J = 1.3 Hz, H-10), 6.88 (td, 1H, 3J = 7.5 Hz; 4J = 1.3 Hz, H-8), 7.03 (dd, 1H, 3J = 7.5 Hz; 4J = 1.6 Hz, H-7), 7.06 (td, 1H, 3J = 7.5 Hz; 4J = 1.6 Hz, H-9); ^{13}C NMR (151 MHz, CD_2Cl_2), δ : 25.4 (C-4), 29.3 (C-3), 3.6 (C-5), 32.2 (C-6), 51.3 (C-2), 122.6 (C-8 and C-10), 127.4 (C-9), 130.9 (C-7), 134.8 (C-6a), 148.2 (C-10a); MS m/z = 161 [M^+]; Anal. calcd for $\text{C}_{11}\text{H}_{13}\text{N}$: C, 81.94; H, 9.38; N, 8.69; Found: C, 81.99; H, 9.33; N, 8.88.

1-Methyl-1,2,3,4,5,6-hexahydrobenzo[b]azocine (1b). Using 0.47 g (2.5 mmol, 1 equiv) 1-methyl-3,4,5,6-tetrahydro-1H-benzo[b]azocin-2-one and 0.19 g (5.0 mmol, 2 equiv) LiAlH_4 provided compound **1b** (0.37 g, 86%) as a colorless oil; bp 66 °C/0.05 mmHg (lit.¹⁴ bp 135–145 °C/14 mmHg); R_f = 0.86 (Al_2O_3 /dichloromethane); IR (ATR): 3059, 3019, 2919, 2846, 2791, 1492, 1445, 1288, 1181, 1109, 748 cm^{-1} ; ^1H NMR (600 MHz, CD_2Cl_2), δ : 1.18–1.21 (m, 2H, H-3), 1.60–1.67 (m, 4H, H-4, H-5), 2.74–2.76 (m, 5H, H-2, H-11), 2.75 (t, 2H, 3J = 5.5 Hz, H-6), 7.02–7.04 and 7.16–7.19 (td, 1H, 3J = 7.6 Hz, 4J = 2.5 Hz and m, 2H; H-8, H-9, H-10), 7.13 (d, 1H, 3J = 7.4 Hz, H-7); ^{13}C NMR (151 MHz, CD_2Cl_2), δ : 27.5 (C-3), 28.8 (C-4), 32.9 (C-6), 33.0 (C-5), 44.3 (C-11), 62.6 (C-2), 121.7 (C-10), 125.0 and 127.2 (C-8 and C-9), 129.8 (C-7), 142.7 (C-6a), 151.2 (C-10a); MS m/z = 175 [M^+]; HRMS (ESI-TOF) m/z calcd for $\text{C}_{12}\text{H}_{18}\text{N}$ 176.1439; Found: 176.1451 [$\text{M} + \text{H}^+$].

1-Isopropyl-1,2,3,4,5,6-hexahydrobenzo[b]azocine (1c). Using 0.57 g (2.6 mmol, 1 equiv) 1-isopropyl-3,4,5,6-tetrahydro-1H-benzo[b]azocin-2-one (**4**) and 0.20 g (5.2 mmol, 2 equiv) LiAlH_4 provided compound **1c** (0.50 g, 94%) as a colorless oil; bp 70–76 °C/0.05 mmHg; R_f = 0.82 (Al_2O_3 /dichloromethane); IR (ATR): 3059, 3019, 2965, 2917, 2847, 2796, 1491, 1447, 1178, 747, 563 cm^{-1} ; ^1H NMR

(600 MHz, CD₂Cl₂), δ : 1.05–1.06 (d, 6H, ³J = 6.2 Hz, H-12 and H-13), 1.08–1.11 (m, H-3), 1.58–1.64 (m, 4H, H-4, H-5), 2.79–2.82 (m, 4H, H-2, H-6), 3.28 (septet, 1H, ³J = 6.2 Hz, H-11), 7.06 (td, 1H, ³J = 7.0 Hz, ⁴J = 1.6 Hz, H-8), 7.15 (d, 1H, ³J = 6.3 Hz, H-7), 7.16–7.19 (m, 2H, H-8 and H-10); ¹³C NMR (151 MHz, CD₂Cl₂), δ : 22.6 (C-12 and C-13), 27.2 (C-3), 28.9 (C-4), 33.2 (C-6), 33.5 (C-5), 52.7 (C-11), 56.0 (C-2), 125.0 (C-10), 125.4 (C-8), 127.1 (C-9), 129.4 (C-7), 145.2 (C-6a), 149.9 (C-10a); MS m/z = 203 [M⁺]; HRMS (ESI-TOF) m/z calcd for C₁₄H₂₂N 204.1752; Found: 204.1749 [M + H]⁺.

1,2,3,4,5,6-Hexahydrobenzo[c]azocine (2a). Using 0.20 g (1.1 mmol, 1 equiv) 1,4,5,6-tetrahydro-2H-benzo[c]azocin-3-one and 0.09 g (2.2 mmol, 2 equiv) LiAlH₄ provided compound 2a (0.14 g, 77%) as a colorless oil: bp 62–64 °C/0.05 mmHg (lit.¹⁴ bp 123 °C/15 mmHg); R_f = 0.29 (Al₂O₃/chloroform/methanol 13:1); IR (ATR): 3409, 3014, 2925, 2850, 2799, 2756, 1597, 1472, 1449, 1351, 762 cm⁻¹; ¹H NMR (600 MHz, CD₂Cl₂), δ : 1.50–1.54 (m, 2H, H-4), 1.67–1.71 (m, 2H, H-5), 2.30 (br s, 1H, H-2 (NH)), 2.66 (t, ³J = 4.8 Hz, H-3), 2.85 (t, 2H, ³J = 6.3 Hz, H-6), 3.87 (s, 2H, H-1), 7.11 (dd, 1H, ³J = 6.7 Hz, ⁴J = 1.4 Hz, H-7), 7.16–7.20 (m, 3H, H-8, H-9, H-10); ¹³C NMR (151 MHz, CD₂Cl₂), δ : 29.1 (C-4), 31.3 (C-5), 32.4 (C-6), 46.7 (C-3), 49.7 (C-1), 126.9 and 127.9 (C-8 and C-9), 129.6 and 129.9 (C-7 and C-10), 139.6 (C-6a), 142.0 (C-10a); MS m/z = 161 [M⁺]; HRMS (ESI-TOF) m/z calcd for C₁₁H₁₆N 162.1283; Found: 162.1296 [M + H]⁺.

2-Methyl-1,2,3,4,5,6-hexahydrobenzo[c]azocine (2b). Using 0.17 g (0.9 mmol, 1 equiv) 2-methyl-1,4,5,6-tetrahydro-2H-benzo[c]azocin-3-one and 0.07 g (1.8 mmol, 2 equiv) LiAlH₄ provided compound 2b (0.13 g, 81%) as a colorless oil: bp 66 °C/0.05 mmHg (lit.¹⁶ bp 114–116.5 °C/4.5–5.4 mmHg); R_f = 0.25 (Al₂O₃/chloroform); IR (ATR): 3060, 2922, 2848, 2790, 1472, 1446, 1043, 751, 717 cm⁻¹; ¹H NMR (600 MHz, CD₂Cl₂), δ : 1.54–1.58 (m, 2H, H-4), 1.65–1.69 (m, H-5), 2.32 (s, 3H, H-11), 2.41 (t, 2H, ³J = 5.0 Hz, H-3), 2.83 (t, 2H, ³J = 6.2 Hz, H-6), 3.73 (s, 2H, H-1), 7.12–7.13 (m, 2H, H-7 and H-10), 7.16 (td, 1H, ³J = 7.2 Hz, ⁴J = 1.5 Hz, H-9), 7.19 (td, 1H, ³J = 7.2 Hz, ⁴J = 1.8 Hz, H-8); ¹³C NMR (151 MHz, CD₂Cl₂), δ : 23.9 (C-4), 31.3 (C-5), 33.3 (C-6), 43.7 (C-11), 54.5 (C-3), 56.3 (C-1), 126.1 (C-9), 128.0 (C-9), 129.9 and 131.2 (C-7 and C-10), 135.2 (C-10a), 142.6 (C-6a); MS m/z = 175 [M⁺]; HRMS (ESI-TOF) m/z calcd for C₁₂H₁₈N 176.1439; Found: 176.1449 [M + H]⁺.

2-Isopropyl-1,2,3,4,5,6-hexahydrobenzo[c]azocine (2c). Using 90 mg (0.4 mmol, 1 equiv) 2-isopropyl-1,4,5,6-tetrahydro-2H-benzo[c]azocin-3-one (5) and 0.30 mg (0.8 mmol, 2 equiv) LiAlH₄ provided compound 2c (50 mg, 60%) as a colorless oil: bp 72–74 °C/0.1 mmHg; R_f = 0.64 (Al₂O₃/ethyl acetate); IR (ATR): 3060, 3016, 2920, 2849, 2803, 1493, 1448, 1360, 1186, 1161, 752, 725 cm⁻¹; ¹H NMR (600 MHz, CD₂Cl₂), δ : 1.11–1.12 (d, 6H, ³J = 6.5 Hz, H-12 and H-13), 1.41–1.45 (m, 2H, H-4), 1.66 (q, 2H, ³J = 6.3 Hz, H-5), 2.67 (t, 2H, ³J = 5.2 Hz, H-3), 2.92–2.98 (m, 3H, H-6 and H-11), 3.75 (s, 2H, H-1), 7.06 (dd, 1H, ³J = 7.0 Hz, ⁴J = 2.0 Hz, H-7), 7.12–7.16 (m, 3H, H-8, H-9, H-10); ¹³C NMR (151 MHz, CD₂Cl₂), δ : 19.8 (C-12 and C-13), 25.0 (C-4), 30.7 (C-5), 32.1 (C-6), 51.0 (C-3), 53.5 (C-1), 55.0 (C-11), 126.3 and 127.5 (C-9 and C-10), 130.0 and 130.3 (C-7 and C-10), 139.0 (C-10a), 141.7 (C-6a); MS m/z = 203 [M⁺]; HRMS (ESI-TOF) m/z calcd for C₁₄H₂₂N 204.1752; Found: 204.1746 [M + H]⁺.

1,2,3,4,5,6-Hexahydrobenzo[d]azocine (3a). Using 0.25 g (1.4 mmol, 1 equiv) 3,4,5,6-tetrahydro-1H-benzo[d]azocin-2-one and 0.11 g (2.8 mmol, 2 equiv) LiAlH₄ provided compound 3a (0.11 g, 48%) as a colorless oil: bp 68 °C/0.1 mmHg (lit.¹⁴ bp 80–84 °C/1 mmHg); R_f = 0.44 (Al₂O₃/dichloromethane/methanol 11:1); IR (ATR): 3400, 3059, 3015, 2934, 2784, 2727, 2692, 2494, 1583, 1475, 774, 762 cm⁻¹; ¹H NMR (600 MHz, CD₂Cl₂), δ : 1.66–1.70 (m, 2H, H-5), 1.79 (br s, 1H, H-3 (NH)), 2.58 (t, 2H, ³J = 5.7 Hz, H-4), 2.77–2.81 (m, 4H, H-1 and H-2), 2.91 (t, 2H, ³J = 5.5 Hz, H-2), 7.06–7.09 (m, 1H, H-7), 7.10–7.14 (m, 3H, H-8, H-9 and H-10); ¹³C NMR (151 MHz, CD₂Cl₂), δ : 31.7 (C-6), 34.8 (C-5), 36.0 (C-1), 47.6 (C-4), 52.5 (C-2), 126.6 and 126.8 (C-8 and C-9), 129.4 and 129.5 (C-7 and C-10), 140.6 (C-10a), 142.0 (C-6a); MS m/z = 161 [M⁺]; HRMS (ESI-TOF) m/z calcd for C₁₁H₁₆N 162.1283; Found: 162.1303 [M + H]⁺.

3-Methyl-1,2,3,4,5,6-hexahydrobenzo[d]azocine (3b). Using 0.13 g (0.7 mmol, 1 equiv) 3-methyl-3,4,5,6-tetrahydro-1H-benzo[d]azocin-2-one and 0.06 g (1.4 mmol, 2 equiv) LiAlH₄ provided compound 3b (0.09 g, 72%) as a colorless oil: bp 64–66 °C/0.05 mmHg; (lit.¹⁷ bp 80–60–62 °C/0.1 mmHg R_f = 0.21 (Al₂O₃/petroleum ether (40–50)/ethyl acetate 11:1); IR (ATR): 3060, 3014, 2926, 2839, 2791, 1491, 1464, 1375, 1310, 1117, 759 cm⁻¹; ¹H NMR (600 MHz, CDCl₃), δ : 1.71–1.75 (m, 2H, H-5), 2.32 (t, 2H, ³J = 5.6 Hz, H-4), 2.41 (s, 3H, H-11), 2.76 (dd, 2H, ³J = 6.7 Hz, ³J = 4.1 Hz, H-2), 2.83 (t, 2H, ³J = 6.5 Hz, H-6), 2.87 (t, 2H, ³J = 5.3 Hz, H-1), 7.09–7.12 (m, 2H, H-7 and H-10), 7.14–7.18 (m, 2H, H-8 and H-9); ¹³C NMR (151 MHz, CDCl₃), δ : 31.0 (C-6), 31.6 (C-5), 34.7 (C-1), 47.2 (C-11), 54.4 (C-4), 61.4 (C-2), 126.4 and 126.8 (C-8 and C-9), 128.9 (C-7), 129.2 (C-10), 140.4 (C-10a), 140.5 (C-6a); MS m/z = 175 [M⁺]; HRMS (ESI-TOF) m/z calcd for C₁₂H₁₈N 176.1439; Found: 176.1449 [M + H]⁺.

3-Isopropyl-1,2,3,4,5,6-hexahydrobenzo[d]azocine (3c). Using 0.11 g (0.5 mmol, 1 equiv) 3-isopropyl-3,4,5,6-tetrahydro-1H-benzo[d]azocin-2-one (6) and 0.04 g (1.0 mmol, 2 equiv) LiAlH₄ provided compound 3c (0.07 g, 70%) as a colorless oil: bp 70–72 °C/0.05 mmHg; R_f = 0.73 (Al₂O₃/petroleum ether (40–50)/ethyl acetate 5:1); IR (ATR): 3060, 3014, 2960, 2927, 2865, 2841, 2804, 1490, 1381, 1359, 1166, 757 cm⁻¹; ¹H NMR (600 MHz, CDCl₃), δ : 0.94 (d, 6H, ³J = 6.6 Hz, H-12 and H-13), 1.53 (br q, 2H, ³J = 5.5 Hz, H-5), 2.15 (t, 2H, ³J = 5.0 Hz, H-4), 2.71 (t, 2H, ³J = 4.7 Hz, H-2), 2.81–2.88 (m, 5H, H-1, H-6 and H-11), 7.06 (dd, 1H, ³J = 6.7 Hz, ⁴J = 2.3 Hz, H-10), 7.09 (dd, 1H, ³J = 6.5 Hz, ⁴J = 2.5 Hz, H-7), 7.11–7.15 (m, 2H, H-8 and H-9); ¹³C NMR (151 MHz, CDCl₃), δ : 18.6 (C-12 and C-13), 30.6 (C-6), 33.5 (C-5), 36.6 (C-1), 47.1 (C-4), 56.0 (C-2 and C-11), 126.0 and 126.4 (C-8 and C-9), 128.8 (C-7), 129.1 (C-10), 141.1 and 141.2 (C-6a and C-10a); MS m/z = 203 [M⁺]; HRMS (ESI-TOF) m/z calcd for C₁₄H₂₂N 204.1752; Found: 204.1750 [M + H]⁺.

NMR Measurements. ¹H and ¹³C NMR spectra were recorded at 600.26/150.94 MHz for 5 mg/mL solutions in CD₂Cl₂ for low-temperature measurements. The ¹H and ¹³C chemical shifts were referenced to TMS as the internal standard. Temperature calibrations were performed using the temperature dependency of the observed chemical-shift separation between the OH resonances and CH_n resonances in methanol for low temperature. The uncertainty in the temperatures was estimated from the calibration curve to be ± 1 K. The COSY, HSQC, and HMBC spectra were recorded using standard procedures and were used to confirm the NMR peak assignments.

Calculation of Energy Barriers. For the estimation of the energy barrier for the inversion process, line shape simulation has been performed using the dynamic ¹H NMR (DNMR) program of the TopSpin package,¹⁴ which allowed the calculation of rate constants. Using the Eyring equation, the free enthalpy of activation (ΔG^\ddagger) was calculated (Supporting Information Figures S45–S52). Based on the equations described by Strondstöm,¹⁸ the energetic barrier of interconversion process between two different conformers were calculated.

Computational Methods. The conformational search of compounds 1–3 was explored using the molecular mechanics MM +.¹⁹ For the found energy minima, further geometry optimization with the Gaussian 09 program²⁰ using DFT with the hybrid B3LYP functional and 6-311G++(d,p) basis set was performed. Energy minima were confirmed by vibrational analysis, which did not show imaginary frequencies and were not scaled. The same combination of functional and basis set was used for ¹H and ¹³C shielding and coupling constants calculation, which were done with GIAO methods and IEF-PCM model solvent (dichloromethane).²¹ The isotropic shielding constants were scaled into chemical shifts using the equation $\delta_{\text{calcd}} = (\sigma_{\text{calcd}} - b)/a$ from the linear regression of the calculated isotropic shielding (σ_{calcd}) against the experimental chemical shift values (δ_{expt}).²² The calculated GIAO isotropic chemical shifts and experimental data for proton and carbon nuclei are presented in Supporting Information Tables S11–S27. The δ values obtained from proton and carbon spectra were compared with calculated chemical shifts. Agreement between the calculated and experimental chemical shifts was evaluated on the basis of the following parameters: the

maximum ($\Delta\delta_{\max}$) and average ($\Delta\delta_{\text{avg}}$) value of the modules of chemical shifts difference and correlation coefficient r^2 .

■ ASSOCIATED CONTENT

● Supporting Information

The Supporting Information is available free of charge on the ACS Publications website at DOI: 10.1021/acs.joc.5b01687.

^1H and ^{13}C NMR spectra of compounds 1–6 at 300 K, VT-NMR spectra (Figures S25–S42). HSQC spectrum of molecules 3a and 3b (Figures S43 and S44). Fitted line shapes of the protons, the calculated rate constants from the DNMR (Figures S45–S52). The computed structures of 2a–c and 3a–c (Figures S53–S58). The values of torsion angles of conformers of *cis*-cyclooctene (Table S1). Electronic energies, enthalpies, free energies, torsion angles of investigated compounds (Tables S2–S10). Comparison of experimental and calculated ^1H and ^{13}C chemical shifts (Tables S11–S27). Total electronic energies, and atomic coordinates from DFT calculations (Tables S28–S69) (PDF)

■ AUTHOR INFORMATION

Corresponding Author

*E-mail: rys@chemia.uj.edu.pl.

Notes

The authors declare no competing financial interest.

■ ACKNOWLEDGMENTS

This study was supported by the Funds for the Statutory Activity of the Faculty of Chemistry of the Jagiellonian University and in part by the PL-Grid Infrastructure. The research was carried out with the equipment purchased thanks to the financial support of the European Regional Development Fund within the framework of the Polish Innovation Economy Operational Program (contract no. POIG.02.01.00-12-023/08).

■ REFERENCES

- (1) Casy, A. F.; Parfitt, R. T. *Opioid Analgesics* 1986, 153–214.
- (2) Klohs, M. W.; Draper, M. S.; Petracek, F. J.; Ginzler, K. H.; Re, O. N. *Arzneim. Forsch.* 1972, 22, 132–133.
- (3) (a) Uchida, L.; Takase, S.; Kayakiri, H.; Kiyoto, S.; Hashimoto, M. *J. Am. Chem. Soc.* 1987, 109, 4108–4109. (b) Kiyoto, S.; Shibata, T.; Yamashita, M.; Komori, T.; Okuhara, M.; Terano, H.; Kohsaka, M.; Aoki, H.; Imanaka, H. *J. Antibiot.* 1987, 40, 594–599. (c) Hirai, O.; Shimomura, K.; Mizota, T.; Matsumoto, S.; Mori, J.; Kikuchi, H. *J. Antibiot.* 1987, 40, 607–611. (d) Shimomura, K.; Hirai, O.; Mizota, T.; Matsumoto, S.; Mori, J.; Shibayama, F.; Kikuchi, H. *J. Antibiot.* 1987, 40, 600–606. (e) Masuda, K.; Nakamura, T.; Mizota, T.; Mori, J.; Shimomura, K. *Cancer Res.* 1988, 48, 5172–5177. (f) Naoe, Y.; Inami, M.; Matsumoto, S.; Nishigaki, F.; Tsujimoto, S.; Kawamura, L.; Miyayasu, K.; Manda, T.; Shimomura, K. *Cancer Chemother. Pharmacol.* 1998, 42, 31–36.
- (4) (a) Seto, M.; Aikawa, A.; Miyomatao, N.; Aramaki, Y.; Kanzaki, N.; Takashima, K.; Kuze, Y.; Izawata, Y.; Baba, M.; Shiraiishi, M. *J. Med. Chem.* 2006, 49, 2037–2048. (b) Lalezari, J.; Gathe, J.; Brinson, C.; Thompson, M.; Cohen, C.; Dejesus, E.; Galindez, J.; Ernst, J. A.; Martin, D. E.; Palleja, S. M. *JAIDS, J. Acquired Immune Defic. Syndr.* 2011, 57, 118–125. (c) Marier, J.-F.; Trinh, M.; Pheng, L. H.; Palleja, S. M.; Martin, D. E. *Antimicrob. Agents Chemother.* 2011, 55, 2768–2774. (d) Baba, M.; Miyake, H.; Wang, X.; Okamoto, M.; Takashima, K. *Antimicrob. Agents Chemother.* 2007, 51, 707–715.
- (5) Anet, F. A. L.; Degen, P. J.; Yavari, I. *J. Org. Chem.* 1978, 43, 3021–3023.
- (6) (a) Lambert, J. B.; Khan, S. A. *J. Org. Chem.* 1975, 40, 369–374. (b) Cameron, S. T.; Scheeren, H. W. *J. Chem. Soc., Chem. Commun.* 1977, 939–941.
- (7) (a) Witosińska, A.; Musielak, B.; Serda, P.; Owińska, M.; Rys, B. *J. Org. Chem.* 2012, 77, 9784–9794. (b) King, F. D.; Aliev, A. E.; Caddick, S.; Tocher, D. A.; Courtier-Murias, D. *Org. Biomol. Chem.* 2009, 7, 167–177. (c) Hassner, A.; Amit, B.; Marks, V.; Gottlieb, H. E. *Eur. J. Org. Chem.* 2006, 2006, 1256–1261.
- (8) Qadir, M.; Cobb, J.; Shelldrake, P. W.; Whittall, N.; White, A. J. P.; Hii, K. K.; Horton, P. N.; Hursthouse, M. B. *J. Org. Chem.* 2005, 70, 1552–1557.
- (9) (a) Renaud, R. N.; Layton, R. B.; Fraser, R. R. *Can. J. Chem.* 1973, 51, 3380–3385. (b) Fraser, R. R.; Layton, R. B.; Raza, M. A.; Renaud, R. N. *Can. J. Chem.* 1975, 53, 167–176. (c) Crossley, R.; Downing, A. P.; Norgadi, M.; Braga de Oliveira, A.; Ollis, W. D.; Sutherland, I. O. *J. Chem. Soc., Perkin Trans. 1* 1973, 205–217.
- (10) Glaser, R.; Ergaz, I.; Leci-Ruso, G.; Shiftan, D.; Novoselsky, A.; Gersh, S. *Annual Reports on NMR Spectroscopy*; Elsevier: London, 2005; Vol 56, pp 141–211 10.1016/S0066-4103(05)56003-4.
- (11) Johenstone, R. A. W.; Rose, M. E. *Tetrahedron* 1979, 35, 2169–2173.
- (12) Hendrickson, J. B. *J. Am. Chem. Soc.* 1967, 89, 7047–7061.
- (13) (a) Ermer, O.; Lifson, S. *J. Am. Chem. Soc.* 1973, 95, 4121–4132. (b) Favini, G.; Buemi, G.; Raimondi, M. *J. Mol. Struct.* 1968, 2, 137–148. (c) Allinger, N. L.; Sprague, J. T. *J. Am. Chem. Soc.* 1972, 94, 5734–5747. (d) Ergaz, I. Ph.D. Dissertation, Ben-Gurion University of the Negev, 2005.
- (14) *TopSpin*, version 3.0; Bruker: Billerica, MA, 2010.
- (15) Koening, H.; Huisegen, R. *Chem. Ber.* 1959, 92, 428–440.
- (16) Jones, G. C.; Hauser, C. R. *J. Org. Chem.* 1962, 27, 3572–3576.
- (17) Kesser, S. V.; Singh, P.; Singh, K. N.; Venugopalan, P.; Kaur, A.; Mahendru, M.; Kapoor, R. *Tetrahedron Lett.* 2005, 46, 6753–6755.
- (18) Sandström, J. *Dynamic NMR Spectroscopy*; Academic Press, London, 1982.
- (19) *HyperChem Professional*, version 8; Hypercube Inc.: Gainesville, FL, 2010.
- (20) Frisch, M. J.; Trucks, G. W.; Schlegel, H. B.; Scuseria, G. E.; Robb, M. A.; Cheeseman, J. R.; Scalmani, G.; Barone, V.; Mennucci, B.; Petersson, G. A.; Nakatsuji, H.; Caricato, M.; Li, X.; Hratchian, H. P.; Izmaylov, A. F.; Bloino, J.; Zheng, G.; Sonnenberg, J. L.; Hada, M.; Ehara, M.; Toyota, K.; Fukuda, R.; Hasegawa, J.; Ishida, M.; Nakajima, T.; Honda, Y.; Kitao, O.; Nakai, H.; Vreven, T.; Montgomery, J. A., Jr.; Peralta, J. E.; Ogliaro, F.; Bearpark, M.; Heyd, J. J.; Brothers, E.; Kudin, K. N.; Staroverov, V. N.; Kobayashi, R.; Normand, J.; Raghavachari, K.; Rendell, A.; Burant, J. C.; Iyengar, S. S.; Tomasi, J.; Cossi, M.; Rega, N.; Millam, J. M.; Klene, M.; Knox, J. E.; Cross, J. B.; Bakken, V.; Adamo, C.; Jaramillo, J.; Gomperts, R.; Stratmann, R. E.; Yazyev, O.; Austin, A. J.; Cammi, R.; Pomelli, C.; Ochterski, J. W.; Martin, R. L.; Morokuma, K.; Zakrzewski, V. G.; Voth, G. A.; Salvador, P.; Dannenberg, J. J.; Dapprich, S.; Daniels, A. D.; Farkas, O.; Foresman, J. B.; Ortiz, J. V.; Cioslowski, J.; Fox, D. J. *Gaussian 09*, revision A.02; Gaussian, Inc.: Wallingford, CT, 2009.
- (21) Tomasi, J.; Mennucci, B.; Cancès, E. *J. Mol. Struct.: THEOCHEM* 1999, 464, 211–226.
- (22) (a) Bagno, A.; Rastrelli, F.; Saielli, G. *Chem. - Eur. J.* 2006, 12, 5514–5525. (b) Costa, F. L. P.; de Albuquerque, A. C. F.; dos Santos, F. M.; de Amorim, M. B. *J. Phys. Org. Chem.* 2010, 23, 972–977. (c) Lodewyk, M. W.; Siebert, M. R.; Tantillo, D. J. *Chem. Rev.* 2012, 112, 1839–1862.